JARO 14: 213–231 (2013)
DOI: 10.1007/s10162-012-0366-8

JARO
Journal of the Association for Research in Otolaryngology

Research Article

Current Steering with Partial Tripolar Stimulation Mode in Cochlear Implants

Ching-Chih Wu[1] and Xin Luo[2]

[1]*School of Electrical and Computer Engineering, Purdue University, 465 Northwestern Avenue, West Lafayette, IN 47907, USA*
[2]*Department of Speech, Language, and Hearing Sciences, Purdue University, 500 Oval Drive, West Lafayette, IN 47907, USA*

Received: 4 March 2012; Accepted: 2 December 2012; Online publication: 19 December 2012

ABSTRACT

The large spread of excitation is a major cause of poor spectral resolution for cochlear implant (CI) users. Partial tripolar (pTP) mode has been proposed to reduce current spread by returning an equally distributed fraction ($0.5\times\sigma$) of current to two flanking electrodes and the rest to an extra-cochlear ground. This study tested the efficacy of incorporating current steering into pTP mode to add spectral channels. Different proportions of current [$\alpha\times\sigma$ and $(1-\alpha)\times\sigma$] were returned to the basal and apical flanking electrodes respectively to shape the electric field. Loudness and pitch perception with α from 0 to 1 in steps of 0.1 was simulated with a computational model of CI stimulation and tested on the apical, middle, and basal electrodes of six CI subjects. The highest σ allowing for full loudness growth within the implant compliance limit was chosen for each main electrode. Pitch ranking was measured between pairs of loudness-balanced steered pTP stimuli with an α interval of 0.1 at the most comfortable level. Results demonstrated that steered pTP stimuli with α around 0.5 required more current to achieve equal loudness than those with α around 0 or 1, maybe due to more focused excitation patterns. Subjects usually perceived decreasing pitches as α increased from 0 to 1, somewhat consistent with the apical shift of the center of gravity of excitation pattern in the model. Pitch discrimination was not better with α around 0.5 than with α around 0 or 1, except for some subjects and electrodes. For three subjects with better pitch discrimination, about half of the pitch ranges of two adjacent main electrodes overlapped with each other in steered pTP mode. These results suggest that current steering with focused pTP mode may improve spectral resolution and pitch perception with CIs.

Keywords: cochlear implant, place pitch, current steering, current focusing, tripolar mode

INTRODUCTION

Cochlear implants (CIs) can partially restore hearing sensation to profoundly deaf people without retrocochlear problems by electrically stimulating the remaining auditory neurons. However, the spectral information encoded for only 12–22 implanted electrodes is limited for high-level auditory processing. The large current spread of monopolar (MP) stimulation (Fig. 1A) causes neural interaction between stimulation sites and further reduces the spectral resolution with CIs. The lack of fine spectral details such as pitch cues makes it difficult for CI users to perceive speech prosody, music melody, and speech in noise (e.g., Zeng 2004). Electric field shaping techniques, such as current focusing and steering, have been proposed to increase the number of distinct perceptual channels in CIs (e.g., Bonham and Litvak 2008).

Current focusing decreases the current spread associated with the main electrode to increase the stimulation selectivity. Unlike MP mode that returns the current to an extra-cochlear ground, full bipolar (BP) mode returns the current to an intra-cochlear adjacent electrode (e.g., the basal flanking electrode in Fig. 1B) to shorten the current return path.

Correspondence to: Xin Luo · Department of Speech, Language, and Hearing Sciences · Purdue University · 500 Oval Drive, West Lafayette, IN 47907, USA. Telephone: +1-765-4967267; fax: +1-765-4940771; email: luo5@purdue.edu

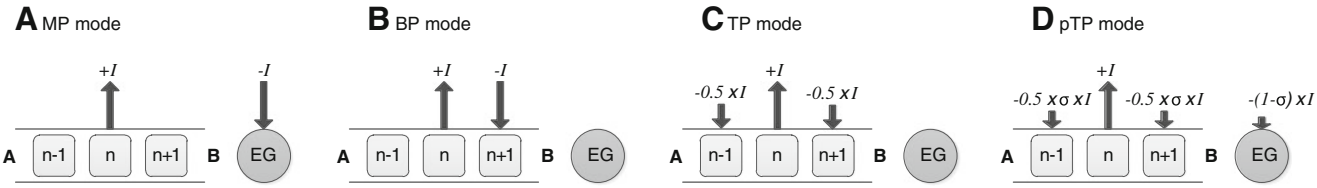

FIG. 1. Schematic illustration of stimulation modes with a fixed current level *I* on the main electrode *n*. The *arrowhead direction* indicates the phases of biphasic current pulses (*upward*: cathodic-leading; *downward*: anodic-leading), while the *arrow length* indicates the current level. *A* apex, *B* base, and *EG* extracochlear ground. **A** Monopolar (MP) mode: the current $-I$ is fully returned to the EG. **B** Bipolar (BP) mode: the current $-I$ is fully returned to the basal or apical (not shown) flanking electrode. **C** Tripolar (TP) mode: the current $-I$ is split and returned evenly to both flanking electrodes. **D** Partial tripolar (pTP) mode: only a fraction of the current ($-\sigma\times I$) is split and returned evenly to both flanking electrodes, while the rest $[-(1-\sigma)\times I]$ to the EG. Note that these plots differ in the current return pathways.

Further, full tripolar (TP) mode (Fig. 1C) returns the current evenly to two intra-cochlear flanking electrodes to limit the current spread on both sides of the main electrode. The intra-cochlear electric field is narrower, and channel interaction is reduced with full TP stimulation compared to full BP or MP stimulation in animal models (e.g., Kral et al. 1998; Bierer and Middlebrooks 2002, 2004; Snyder et al. 2004) and human CI listeners (e.g., Bierer 2007; Bierer and Faulkner 2010; Landsberger et al. 2012). With a smaller population of excited neurons, the focused full TP stimulation requires more current to reach the most table level and sometimes cannot support full loudness growth or cover the entire dynamic range within the compliance limit of the implant, especially for patients with high electrode impedances. To address the loudness issue while keeping the stimulation focused, partial tripolar (pTP) mode (Fig. 1D) has been proposed to return only part of the current to the flanking electrodes (controlled by the compensation coefficient σ). The stimulation mode changes from full MP to full TP as σ varies from 0 to 1. Although spectral ripple discrimination improved with σ=0.75, speech recognition was similar with pTP or MP stimulation (Berenstein et al. 2008). With focused pTP mode, CI users were more susceptible to poor electrode–neuron interface (Bierer 2010), which may adversely affect the perception of certain frequency information. Besides, the compensation coefficient σ may need optimization for different subjects and electrodes, so that the most focused pTP stimulation with full loudness growth could be utilized. Finally, while the stimulation on each main electrode was narrowed by pTP mode (e.g., Landsberger et al. 2012), the number of physical electrodes was still not enough to resolve fine spectral details such as the low-order harmonics of fundamental frequency, which have been shown by Qin and Oxenham (2005) to be important for speech recognition in noise and melody recognition.

Current steering changes the peak or centroid of neuron activation to be located between adjacent electrodes, so that the number of frequency channels could be increased beyond the number of physical electrodes. In the MP-mode current steering (Fig. 2A), a fixed amount of current was steered between two adjacent main electrodes, and the fraction of current on the basal main electrode of the pair was controlled by a steering coefficient α. Higher pitch percepts were elicited with increasing α (i.e., more current injected to the basal main electrode). CI users perceived on average five intermediate pitch sensations per electrode pair (e.g., Donaldson et al. 2005), but their speech recognition only slightly improved with speech processing strategies using the MP-mode current steering (e.g., Firszt et al. 2009). The large current spread of MP stimulation may have limited the number of independent spectral channels with MP-mode current steering. Current steering has also been implemented in partial bipolar (pBP) mode or with the phantom-electrode stimulation (Saoji and Litvak 2010), which returns a fraction (σ) of current to the basal flanking electrode (Fig. 2B). Lower pitch percepts were elicited with increasing σ (i.e., more current returned to the basal flanking electrode). However, pitch reversal occurred for some subjects as σ neared 1 and the stimulation side lobe around the basal flanking electrode became perceptually salient.

In this study, current steering with focused pTP mode (Fig. 2C) was proposed to increase the spectral or pitch cues for CI users. With a fixed compensation coefficient σ, steered pTP mode distributes the intracochlear return current to the basal and apical flanking electrodes with a proportion of α (the steering coefficient) and $1-\alpha$, respectively. With the basal and apical current spread limited to different degrees, the location of the peak or centroid of the excitation pattern can be changed to elicit different pitch percepts. The standard pTP mode (Fig. 1D) can be seen as a special case of steered pTP mode with α=0.5. When the intra-cochlear return current is distributed to either the basal (α=1; Fig. 2B) or apical

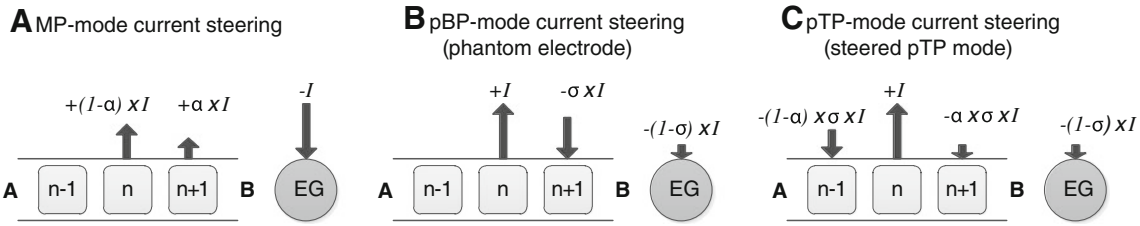

FIG. 2. Schematic illustration of current steering in MP, partial BP (pBP), and pTP modes. Refer to Figure 1 for annotations. **A** MP-mode current steering: two adjacent main electrodes are simultaneously stimulated in phase with varying ratios of current level (α and $1-\alpha$ on the basal and apical electrodes, respectively). **B** pBP-mode current steering or phantom electrode: a fraction of the current ($-\sigma\times I$) is returned to the basal or apical (not shown) flanking electrode and the rest $[-(1-\sigma)\times I]$ to the EG. **C** pTP-mode current steering or steered pTP mode: a fraction of the current ($-\sigma\times I$) is split and returned to the basal and apical flanking electrodes with ratios of α and $1-\alpha$, respectively, and the rest $[-(1-\sigma)\times I]$ to the EG.

flanking electrode alone (α=0), steered pTP mode is equivalent to pBP mode. Based on the results of phantom electrodes (Saoji and Litvak 2010), steered pTP mode was expected to elicit lower pitch percepts with increasing α (i.e., more current returned to the basal flanking electrode). Because standard pTP stimulation may be more focused than pBP stimulation, we also hypothesized that pitch discrimination would be better and the current required for equal loudness would be higher with α=0.5 than with α=0 or 1. Table 1 summarizes the various stimulation configurations achievable with steered pTP mode using different combinations of α and σ.

A computational model that simulates intra-cochlear potential fields and auditory neural response to CI stimulation (Goldwyn et al. 2010) was used to investigate loudness and pitch perception with steered pTP mode. Similar models have been used to study loudness growth with standard pTP stimulation (Litvak et al. 2007) and simulate current focusing and steering in various modes (Bonham and Litvak 2008). Modeling studies were less time-consuming than testing human CI subjects and could provide valuable insights into human perceptual data, thanks to their capability of adjusting specific CI factors and examining conditions that were difficult to test in real CI users. However, a number of simplifying assumptions were necessary for a model to be computationally tractable. It was thus important to validate the model by other objective measures or psychophysical tests. As such, two psychophysical experiments with CI users were also conducted to investigate steered pTP mode. In experiment 1, steered pTP stimuli with α from 0 to 1 on a main electrode were balanced in loudness and then ranked in pitch. Experiment 2 compared the pitches of loudness-balanced steered pTP stimuli on adjacent main electrodes to estimate the overlap between their pitch ranges.

COMPUTATIONAL MODEL

Figure 3 depicts the model of Goldwyn et al. (2010), which simulates the spatial pattern of neural activity along the cochlea in response to CI stimulation. The model is briefly described here, and more details can be found in Goldwyn et al. (2010). In this model, the scala tympani is simplified as a 33-mm subsection of an infinitely long cylinder with a fixed radius of 1 mm. The resistivity of the surrounding osseous spiral lamina is about a hundred times greater than that inside the fluid-filled scala tympani. The spiral ganglion cells are 0.3 mm away from the scala tympani. In case of full neural survival, 330 clusters of 100 spiral ganglion cells are evenly distributed along the cochlea (one cluster per 0.1 mm). A 16-electrode array with an inter-electrode spacing of 1.1 mm is placed in the center of the scala tympani to simulate the HiFocus1J electrode array from Advanced Bionics (Sylmar, CA). The most basal electrode (EL16) is 3 mm from the base of the cochlea. The electrode-neuron distance is

TABLE 1

Stimulation configurations achievable with steered pTP mode using different combinations of α and σ

	σ=0	0<σ<1	σ=1
α=0	MP	Basally shifted pBP	Basally shifted BP
0<α<0.5		Basally shifted pTP	Basally shifted TP
α=0.5		Standard pTP	Standard TP
0.5<α<1		Apically shifted pTP	Apically shifted TP
α=1		Apically shifted pBP	Apically shifted BP

The naming convention of a stimulation configuration is based on the hypothesized shift of its excitation pattern. For example, compared to standard pTP mode, apically shifted pTP mode is expected to elicit lower pitch percepts with increasing α

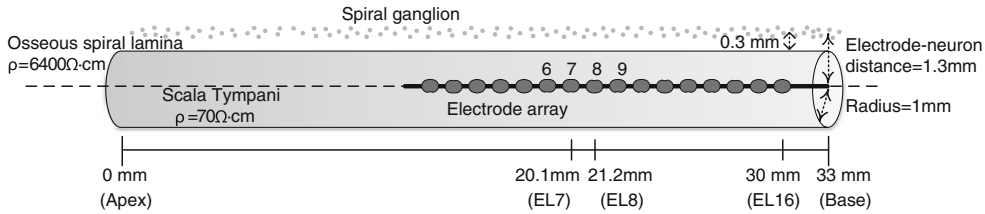

FIG. 3. Schematic illustration of the adapted model (Goldwyn et al. 2010) and its parameters. The scala tympani is modeled by a 33-mm subsection of an infinitely long cylinder with a fixed radius of 1 mm. The resistivity inside the scala tympani (70 Ωcm) is lower than that of the surrounding osseous spiral lamina (6,400 Ωcm). A 16-electrode array with an inter-electrode spacing of 1.1 mm is placed in the center of the scala tympani. The most basal electrode EL16 is 3 mm from the base of the cochlea. Spiral ganglion cells are evenly distributed along the entire length of the cochlea and located in the spiral lamina with a distance of 1.3 mm from the electrode array.

1.3 mm for all electrodes. These parameters were adapted from Goldwyn et al. (2010). Real CI users would have variable neural survival (Nadol et al. 2001) and electrode-neuron distances (Finley and Skinner 2008), but that information was not available and thus was not modeled for the subjects in this study. The inter-subject variability is likely evident in the psychophysical tests.

The first step of model computation is to derive the potential field of CI electric stimulation. For steered pTP mode, the overall potential field is thought to be the linear sum of those of the main and flanking electrodes with the proportional current levels shown in Figure 2C. In our model simulation, the compensation coefficient σ was 0.75 and the steering coefficient α varied from 0 to 1 in steps of 0.1, similar to those used for human subjects in experiments 1 and 2. An activating function (Rattay 1999) is defined as the second spatial derivative of the potential field and was calculated at the midpoint of each neural cluster. The thresholds of neurons within each cluster were approximated by a normal distribution, with the mean and standard deviation determined from human psychophysical data (Goldwyn et al. 2010) and animal studies (Miller et al. 1999), respectively. Together, the activating function value and threshold distribution were used to calculate the number of activated neurons for each cluster. The final output of the computational model was the number of activated neurons as a function of cochlear position (i.e., an excitation pattern).

To simulate equal loudness with different α and to demonstrate the effect of α on the model excitation pattern, a simplifying assumption had to be made for the relation between loudness perception and activated neuron counts. Here, loudness-balanced pTP stimuli with different α were assumed to activate the same number of neurons, as in Goldwyn et al. (2010) and Litvak et al. (2007). Although there was no evidence that a chosen neuron count corresponded to a particular value on a loudness perception scale, the current levels that activated 100 and 1,000 neurons were assumed to be around the perceptual threshold and most comfortable level, respectively.

Simulated excitation patterns with different α

Figure 4 shows the simulated excitation patterns (blue areas) for steered pTP stimuli, which activated a total of 100 (left column) and 1,000 neurons (right column), and were presented on the main electrode EL8 (black arrows) with α varying from 0 to 1 in steps of 0.1 (different rows). The peak (green "+") of excitation pattern was defined as the position of the neural cluster with the maximum number of activated neurons. The center of gravity (CoG; red "*") of excitation pattern was calculated as follows:

$$CoG = \frac{\sum_{i=1}^{330} N_i \times 0.1 \times i}{\sum_{i=1}^{330} N_i}$$

where i is the index of neural cluster, N_i is the number of activated neurons in the ith cluster, and $0.1 \times i$ is the distance from apex for the ith cluster (note that there was one cluster per 0.1 mm). The denominator was the total number of activated neurons across the whole cochlea (i.e., 100 or 1,000 for the assumed threshold or most comfortable level). To quantify the spread of excitation, the bandwidth (bw) of excitation pattern was calculated at 75 % of the peak value. The following sections will discuss the use of peak, CoG, and bandwidth of an excitation pattern to estimate its pitch and loudness perception.

Simulated equal-loudness contours across different α

The current levels on the main electrode (in decibels re 1 μA) needed to activate a total of 100 and 1,000 neurons in the model are plotted as a function of the steering coefficient α in Figure 5. Assuming that loudness-balanced stimuli would activate the same number of neurons, each contour in Figure 5 represents an equal-loudness level with different α (triangles and circles for the assumed threshold and most comfortable level, respectively). Both equal-loudness contours peaked at α=0.5 and monotonically

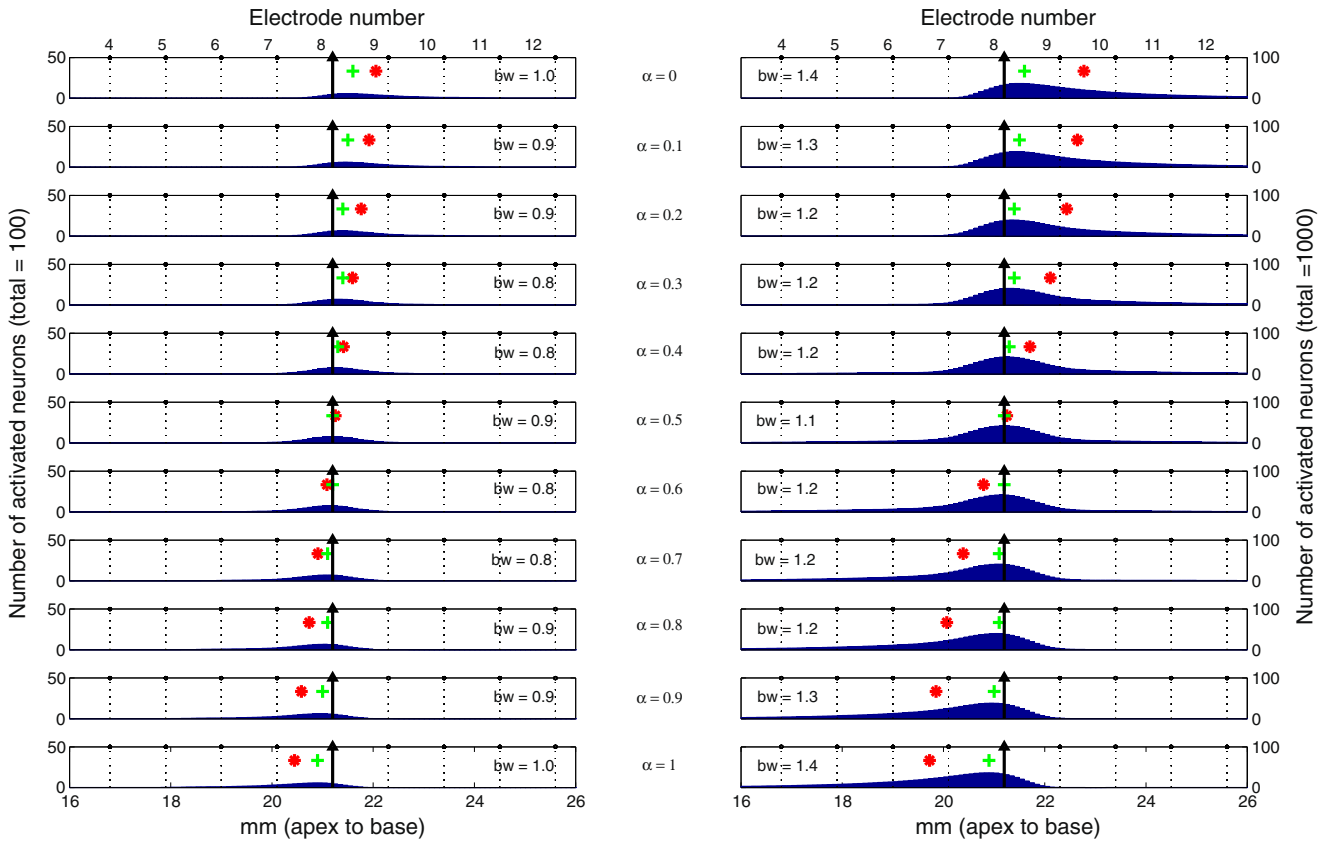

FIG. 4. The number of activated neurons (*blue bars*) calculated from the computational model is displayed as a function of cochlear position for different α (*rows*) and different activated neuron counts (*left column*: 100; *right column*: 1,000). Except for the main electrode (EL8, *black arrow*), electrode positions are shown in *dotted lines* and their numbers are labeled on *top of each column*. Also shown for each excitation pattern are its bandwidth (bw: the width of excitation in millimeters at 75 % peak value) and the location of peak (*green cross*) and centroid (*red asterisk*).

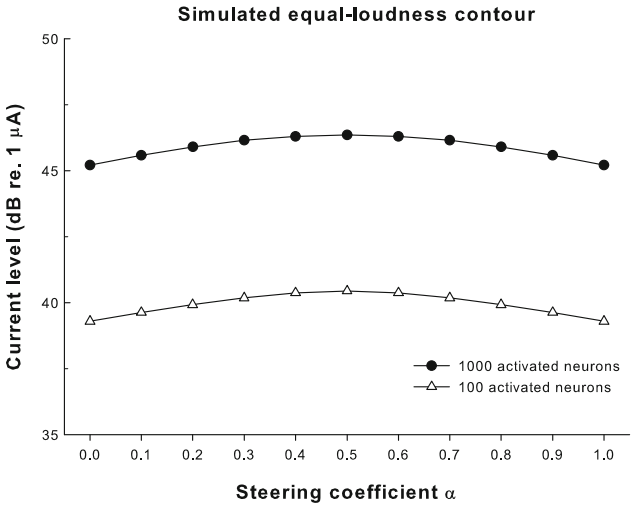

FIG. 5. Current levels (in decibels re 1 μA) required to activate a total of 100 and 1,000 neurons (*open triangles* and *solid circles*, respectively) in the model as a function of the steering coefficient α. The current levels that activated a total of 100 and 1,000 neurons were assumed to be around the perceptual threshold and most comfortable level, respectively.

decreased for higher or lower α. These results may be explained by the spread of excitation with different α (Fig. 4). At both levels, standard pTP mode with α=0.5 reduced current spread on both the apical and basal sides to a similar degree and created a narrow excitation pattern centered on the main electrode. As α approached 0 or 1, the stimulation mode became more like pBP and current spread was more limited on one side of the main electrode than on the other side. The broader excitation patterns for α around 0 or 1 (as indicated by the greater bandwidths of excitation) thus required less current to achieve equal loudness. The two equal-loudness contours were parallel to each other, suggesting that the loudness growth and dynamic range were similar across α.

Simulated pitch changes with α on adjacent main electrodes

Figure 6 shows the simulated place-pitch changes with α in steered pTP mode. The peak (top row) and CoG (bottom row) of excitation pattern at the assumed

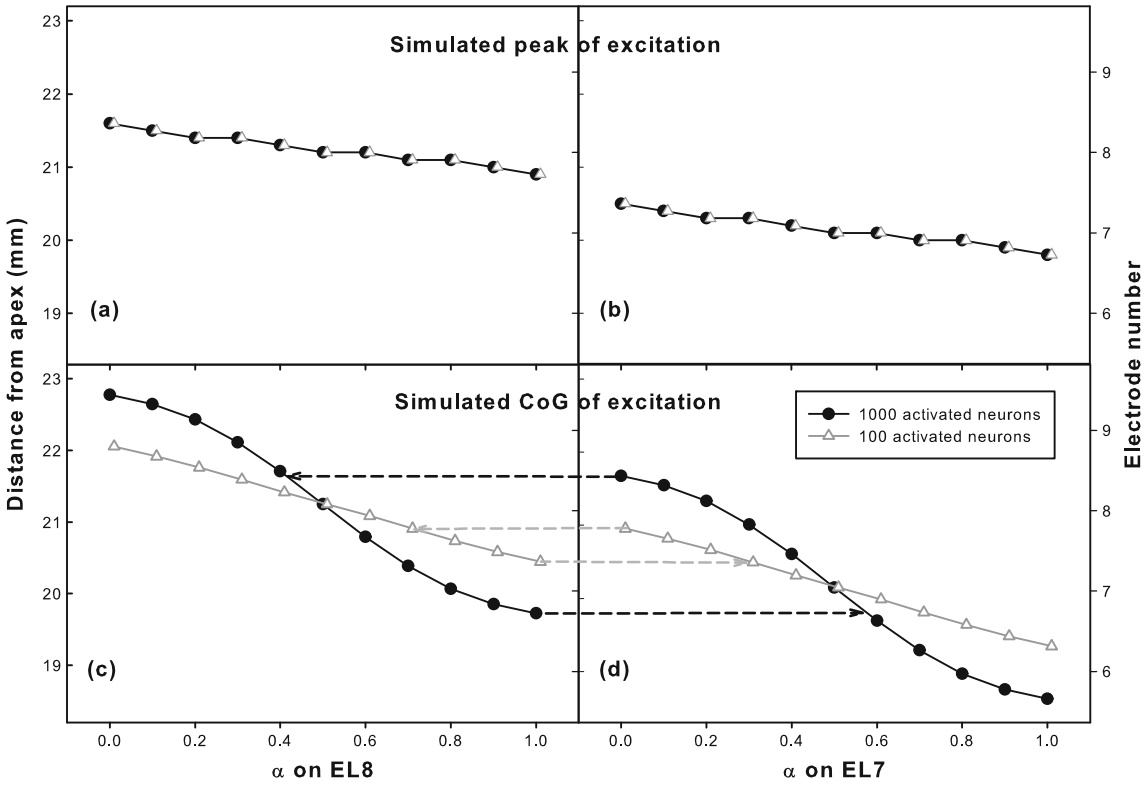

FIG. 6. Peak (*top row*) and center of gravity (CoG; *bottom row*) of simulated excitation pattern for various α on EL8 (*left column*) and EL7 (*right column*) with a total of 100 (*triangles*) and 1,000 activated neurons (*circles*). Due to model simplification, the peak and CoG curves for EL7 were identical to those for EL8 but shifted to the apex by the inter-electrode spacing. For the two adjacent main electrodes, their excitation peaks did not overlap, while their CoGs of excitation overlapped with each other as indicated by the *horizontal dashed lines in the bottom row*.

threshold (triangles) and most comfortable level (circles) are shown against different α on EL8 (left column) and EL7 (right column). Note that in the simplified model, the peak and CoG curves for EL7 were identical to those for EL8 but shifted to the apex by 1.1 mm (i.e., the inter-electrode spacing). When α increased from 0 to 1, the peak of excitation only shifted 0.3 mm to the apex at both levels, while the CoG of excitation greatly shifted about 1.5 and 2.5 mm at the assumed threshold and most comfortable level, respectively. Close inspection of Figure 4 reveals that returning more current to the basal flanking electrode (and less to the apical one) reduced the basal current spread but increased the apical current spread, leading to an apical shift of the overall excitation pattern. Therefore, if place pitch is mostly determined by the CoG of excitation, CI users would perceive lower pitches for higher α, and the pitch changes with steered pTP mode would be more salient at higher stimulation levels. Another effect that can be observed in Figure 6 was that the CoG of excitation at the assumed most comfortable level shifted more rapidly with the same α step of 0.1 when α was around 0.5, indicating better pitch discrimination for more focused pTP stimuli with α around 0.5 than for less focused pBP stimuli with α around 0 or 1. However, this effect was level dependent as the CoG of excitation at the assumed threshold shifted more linearly with α from 0 to 1.

The overlap of pitch ranges between adjacent main electrodes can be predicted by comparing the left and right columns of Figure 6. Although the peaks of excitation for EL7 and EL8 were well separated, their CoGs of excitation greatly overlapped with each other. The pitch overlap estimated by the CoG of excitation was greater at the assumed most comfortable level than at the approximate threshold, as indicated by the horizontal dashed lines connecting Figure 6C and D. At the assumed most comfortable level, the lowest pitch on EL8 with α=1 would be similar to the middle pitch on EL7 with $\alpha \approx 0.6$, and the highest pitch on EL7 with α=0 would be similar to the middle pitch on EL8 with $\alpha \approx 0.4$.

These model predictions of loudness and pitch perception were next tested with human CI subjects, using the same steered pTP stimuli but only at the most comfortable level. Although the modeling showed interesting results near threshold, related

results in human listeners are difficult to obtain due to the time and strain associated with listening to stimuli that are barely audible.

EXPERIMENT 1: PITCH RANKING OF STEERED PTP STIMULI ON A MAIN ELECTRODE

Methods

Subjects and stimuli. Four post-lingually (S1, S2, S4, and S6) and two pre-lingually deafened (S3 and S5) adult CI users participated in experiment 1. Table 2 shows their demographic details and sentence recognition scores obtained during the most recent clinical visit. Percent correct scores for the Hearing in Noise Test (HINT) sentences in quiet at 60 dB SPL were available for all subjects except S5, who only had scores for the City University of New York (CUNY) sentences. Only users of the Advanced Bionics HiRes 90 K implant were recruited because this device can stimulate multiple electrodes simultaneously and allows for the delivery of pTP stimulation. All subjects used the HiFocus1J electrode array with an electrode spacing of 1.1 mm, as simulated in the computational model. This study was reviewed and approved by the Purdue IRB committee. All subjects provided informed consent and were compensated for their participation.

All experimental stimuli were delivered to CI subjects using the Bionic Ear Data Collection System (Advanced Bionics, Sylmar, CA). As defined in Figure 2C, when current I was applied to the main electrode ELn, $-\alpha\times\sigma\times I$ was returned to the basal flanking electrode ELn+1, while $-(1-\alpha)\times\sigma\times I$ was returned to the apical flanking electrode ELn-1. The compensation coefficient σ was selected using the method described in the next section, while the steering coefficient α ranged from 0 to 1 in steps of 0.1. For brevity, $pTP_{ELn,\ \alpha=\alpha 1}$ denotes a steered pTP stimulus on the main electrode ELn with α equal to $\alpha 1$. Pulse trains were 300 ms long with 1,000 pulses per second. The symmetric biphasic pulses (226 μs/phase) were cathodic-leading on the main electrode and anodic-leading on the flanking electrodes. The 226-μs phase duration was longer than those used in the clinic and was chosen to help achieve full loudness growth (up to the upper loudness limit) for pTP stimulation within the compliance limit of the implant (i.e., the voltage on each electrode should be lower than 8 V, and the surface charge density should be lower than 100 $\mu C/cm^2$; Saoji and Litvak 2010). To investigate performance variation across the electrode array, steered pTP stimuli on the apical (EL4), middle (EL8), and basal (EL12) main electrodes were tested. Stimuli on EL12 were not tested for S3 since EL11 to 16 were deactivated in her clinical speech processor. S5 was also not tested on EL12 after she failed in the attempts to balance loudness for several α values on EL12 within the compliance limit of the implant (see the procedure in the "Loudness balancing across different α" section).

Determining the compensation coefficient σ. For each tested main electrode ELn, the highest compensation coefficient σ that allowed for full loudness growth within the compliance limit was chosen. This σ value was expected to keep the overall excitation patterns of pTP stimuli as focused as possible and result in steered pTP mode with the greatest shift and the least channel interaction. During the search for the highest possible σ, the steering coefficient α was fixed at 0.5. Based on model predictions (Fig. 5), for a given σ, $pTP_{ELn,\ \alpha=0.5}$ would have the most focused excitation pattern and require the most current to reach the upper loudness limit among all $pTP_{ELn,\ \alpha=0,\ 0.1,\ \ldots,\ 1}$. Therefore, if full loudness growth was achieved for α=0.5 within the compliance limit, it should also be possible for the other α values. Loudness growth for each tested σ was measured using a clinical 10-point scale (Advanced Bionics, Sylmar, CA) from 1 ("just noticeable") to 10 ("too loud"). Starting from a sub-threshold level, the current level was increased in 8-μA steps until loudness level 9 on the scale ("upper loudness limit") was perceived or the implant compliance limit was reached.

TABLE 2

Subject demographic details

Subject	*Age (years)*	*Years of profound deafness*	*Gender*	*Etiology*	*Processing strategy*	*Years with prosthesis*	*HINT sentence recognition[a] (%)*
S1	82	3	F	Sudden hearing loss	HiRes-P w/Fidelity 120	3	96
S2	62	25	F	Gestational hypertension	HiRes-P	6	88
S3	37	34	F	Spinal meningitis	HiRes-S w/Fidelity 120	2	14
S4	42	N/A	F	Sudden hearing loss	HiRes-P w/Fidelity 120	7	94
S5	60	55	F	Unknown	Emulated CIS	2	N/A
S6	64	19	F	Hereditary deafness	HiRes-P	6	94

[a]The Hearing In Noise Test (HINT) sentences were tested in quiet at 60 dB SPL during the most recent clinical visit. S5 was only tested with the CUNY sentences and scored 14 % correct

The binary search algorithm (Cormen et al. 2009) was used to speed up the search for the highest possible σ. The initial search range for σ was (0, 1), and σ=1 (i.e., the most focused full TP mode) was tested first. If the upper loudness limit could be reached within the compliance limit for σ=1, the search stopped with an output of σ=1. Otherwise, the midpoint of the initial search range (i.e., σ=0.5) was tested. If the upper loudness limit could be reached within the compliance limit for σ=0.5, the search range for σ was limited to the higher half (0.5, 1). Otherwise, the search range for σ was limited to the lower half (0, 0.5). The midpoint of the reduced search range was then tested. This search continued in a similar fashion until the size of the search range was reduced to 0.05 (i.e., the search result had a precision of 0.05). The output of σ was then applied to steered pTP stimuli with different α on the same main electrode. With the found σ, full loudness growth was indeed achieved for each α within the compliance limit, except for several α values on EL12 of S5. The dynamic range (DR) from loudness level 1 (defined as T-level) to 9 (defined as C-level) was measured using the method described above.

Loudness balancing across different α. On each main electrode ELn, pTP stimuli with different α from 0 to 1 in steps of 0.1 were loudness balanced to avoid loudness effects on the next pitch-ranking tests. The reference stimulus was $pTP_{ELn,\ \alpha=0.5}$ at the most comfortable level (M-level: loudness level 6 during the DR measurement), while the target stimulus was $pTP_{ELn,\ \alpha}$ with $\alpha \neq 0.5$. Different α values were tested separately in a random order. As mentioned above, α=0.5 was predicted to require the most current for M-level among all current steering coefficients for steered pTP stimuli. Therefore, using $pTP_{ELn,\ \alpha=0.5}$ as the reference would leave a greater range of current adjustment for the target, so as to improve the reliability of loudness balancing. A two-alternative, forced-choice (2AFC), double-staircase procedure (Jesteadt 1980) was used to balance the loudness of the target and reference. A 2-down/1-up and a 2-up/1-down adaptive sequence were randomly interleaved. In each trial, the reference and target stimuli were presented in a random order. Subjects were asked to choose the louder stimulus regardless of possible pitch and timbre differences. The target current level on the main electrode was adjusted based on subject response using the corresponding adaptive rule and was always limited within the compliance limit. The current level step size was 20 μA for the first four reversals and 12 μA thereafter. Each sequence was terminated after 12 reversals or 60 trials, and the average current level over the last eight reversals and across the two sequences was the loudness-balanced level for the target stimulus. If the number of reversals in a sequence was less than eight after 60 trials, the attempt to balance loudness for the target stimulus failed.

Pitch ranking of steered pTP stimuli. On each main electrode ELn, a 2AFC task was used to compare the pitches of ten consecutive pairs of loudness-balanced steered pTP stimuli with a 0.1 interval in α, ranging from 0 to 1. In each trial, a stimulus pair (e.g., $pTP_{ELn,\ \alpha=0.2}$ vs. $pTP_{ELn,\ \alpha=0.3}$) was randomly chosen, and the stimuli in this pair were presented also in a random order. Amplitude roving of ±0.5 dB was applied to all stimuli to further reduce possible loudness effects. The task of the subject was to indicate which stimulus had higher pitch. Subjects were allowed to repeat the stimuli as many times as desired before responding. No feedback was provided as to the correctness of each response because pitch reversals could occur when the side lobes around the flanking electrodes became perceptually salient (Saoji and Litvak 2010). Twenty trials of each stimulus pair were tested in a run, and data from two runs were averaged. For α=0.1, 0.2, …, 1, the percentages that $pTP_{ELn,\ \alpha}$ was judged as higher in pitch than $pTP_{ELn,\ \alpha-0.1}$ were recorded and converted to d' values (Hacker and Ratcliff 1979) to indicate the perceptual distance or sensitivity index between steered pTP stimuli with an α interval of 0.1. The overall cumulative d', calculated by successively summing the d' values from α=0.1 to α=1, could be used to estimate the overall pitch changes on a main electrode in steered pTP mode.

Results

Subject- and electrode-specific compensation coefficient σ. Figure 7 shows the highest possible compensation coefficient σ that allowed for full loudness growth within the compliance limit for each subject on the

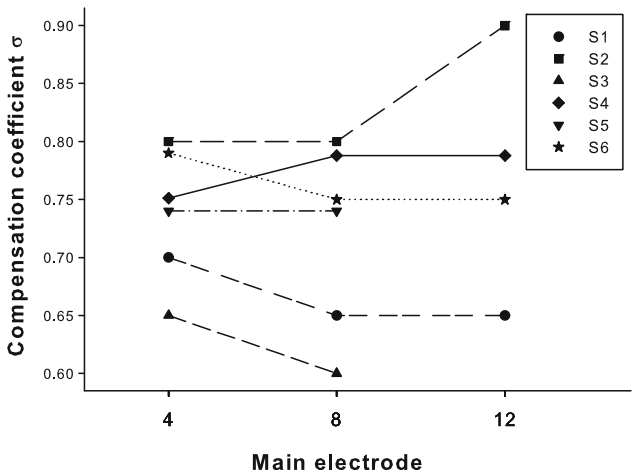

FIG. 7. Compensation coefficient σ for individual subjects (*different symbols and line types*) across the apical (EL4), middle (EL8), and basal (EL12) main electrodes.

three main electrodes. A one-way repeated-measures (RM) analysis of variance (ANOVA) revealed no significant effect of electrode on the highest possible σ ($F_{2,8}$=0.17, p=0.85). The variation of σ across the three electrodes of each subject was usually 0.05 (i.e., equal to the minimum step for σ search), except for S2 who had a variation of 0.1. In contrast, the highest possible σ varied greatly from 0.6 to 0.9 for different subjects.

Dynamic range between T/C levels. Figure 8 shows the DRs (dynamic ranges, denoted by shaded area) between T- (thresholds, denoted by upward triangles) and C-levels (upper loudness limits, denoted by downward triangles) on each main electrode as a function of the steering coefficient α. All current levels are in decibels re 1 μA. The applied compensation coefficient σ is also included in each plot. Two-way RM ANOVAs were performed to analyze the effects of electrode and α on T/C levels and DRs, respectively. Both T-levels and DRs were not significantly affected by either electrode ($F_{2,8}$=3.71, p=0.07 for T-levels; $F_{2,8}$=2.89, p=0.11 for DRs) or α ($F_{10,50}$=0.87, p=0.57 for T-levels; $F_{10,50}$=0.11, p=1.00 for DRs). However, C-levels were significantly affected by both electrode ($F_{2,8}$=9.19, p=0.01) and α ($F_{10,50}$=2.11, p=0.04). There was no significant interaction between electrode and α for T-levels ($F_{20,80}$=0.09, p=1.00), C-levels ($F_{20,80}$=0.33, p=1.00), and DRs ($F_{20,80}$=0.14, p=1.00). Post hoc t tests with Bonferroni correction showed that C-levels were only significantly higher on EL8 than on EL4 (p=0.01), but not significantly different between any α pair. Future examination of neural survival and imaging of electrode placement may help explain the increased C-levels on EL8. Also note that T/C levels of steered pTP stimuli were only measured on three main electrodes, which did not explore the possible threshold variation across the electrode array as shown in Bierer (2007).

Equal-loudness contour at M-level. Figure 8 also shows the equal-loudness contours at the most comfortable level (M-level, denoted by circles) for individual subjects and electrodes. As can be seen, M-levels were well above T-levels but close to C-levels. In a few cases (e.g., $pTP_{EL8,\ \alpha=0.7}$ for S2 and $pTP_{EL12,\ \alpha=0.9}$ for S6), the M-level obtained from loudness balancing across α even exceeded the C-level obtained from loudness growth within α, most likely due to their different methods of measurement (i.e., method of adjustment for M-level and method of limits for T/C levels). The patterns of equal-loudness contours at M-level varied across subjects and electrodes. For EL12 of S2 and all electrodes of S4 and S5, the M-level contours peaked at α around 0.5 and decreased toward both ends at α equal to 0 or 1. For EL8 of S2 and EL4 and EL12 of S6, the M-level contours peaked at α around 0 or 1 and decreased toward the other end. For the other electrodes including those of S1 and S3, the contours of M-level were relatively flat. A two-way RM ANOVA revealed significant effects of both electrode ($F_{2,8}$=18.22, p=0.001) and α ($F_{10,50}$=3.43, p=0.002) on M-levels. Electrode and α did not significantly interact with each other ($F_{20,80}$=0.70, p=0.82). Post hoc Bonferroni t tests showed that M-levels were significantly higher on EL8 than on EL4 (p=0.004) and EL12 (p=0.002), a pattern similar to that of C-levels. As α varied, M-levels were only significantly higher for standard pTP mode with α=0.5 than for pBP mode with α=0 (p=0.03) or 1 (p=0.05). Unlike T/C levels, M-levels were carefully loudness balanced across α using the adaptive procedures and thus may better reflect the different current requirements for different α.

Pitch ranking of steered pTP stimuli. Pitch-ranking results (i.e., the percentages that $pTP_{ELn,\ \alpha}$ was judged as higher in pitch than $pTP_{ELn,\ \alpha-0.1}$, where α=0.1, 0.2, …, 1) were converted to d' values, which are shown in Figure 9 as a function of α (gray circles), with the ordinate for d' labeled on the right. Also shown in Figure 9 are the cumulative d' functions (black circles with the ordinate labeled on the left) across subjects and electrodes. The cumulative d' started from 0 at α=0 and was the summation or running total of successive d' values with increasing α. The cumulative d' at α=1 was called the overall cumulative d' and would be used to derive the number of discriminable pitch steps on a main electrode later.

Positive d' values indicate higher pitches for higher α (with percentages>50 %), while negative d' values indicate lower pitches for higher α (with percentages<50 %). The d' values shown in Figure 9 had a mean of −0.56 and a standard deviation of 0.73, which suggests that for the tested electrodes and α, the perceived pitch of $pTP_{ELn,\ \alpha}$ was usually lower, but occasionally similar or higher, than that of $pTP_{ELn,\ \alpha-0.1}$. This somewhat agrees with the model prediction that higher α pushes the excitation pattern to the apex and results in lower pitch percepts. A two-way RM ANOVA performed on the d' values showed a nearly significant effect of α ($F_{9,45}$=2.03, p=0.06), but not of electrode ($F_{2,8}$=0.62, p=0.56), or their interaction ($F_{18,72}$=0.68, p=0.81).

Since the d' values were mostly negative or close to zero, the cumulative d' was in general a monotonic decreasing function of α for most subjects except S2 and S3. Figure 9 also shows that for some of the tested electrodes (e.g., EL4 and EL8 of S1, EL4 and EL12 of S4), the cumulative d' function decreased faster in the middle than at the two ends of α. However, as revealed by the above analysis of the d' values, the change in cumulative d' with a 0.1 interval in α was not significantly different across α. The overall

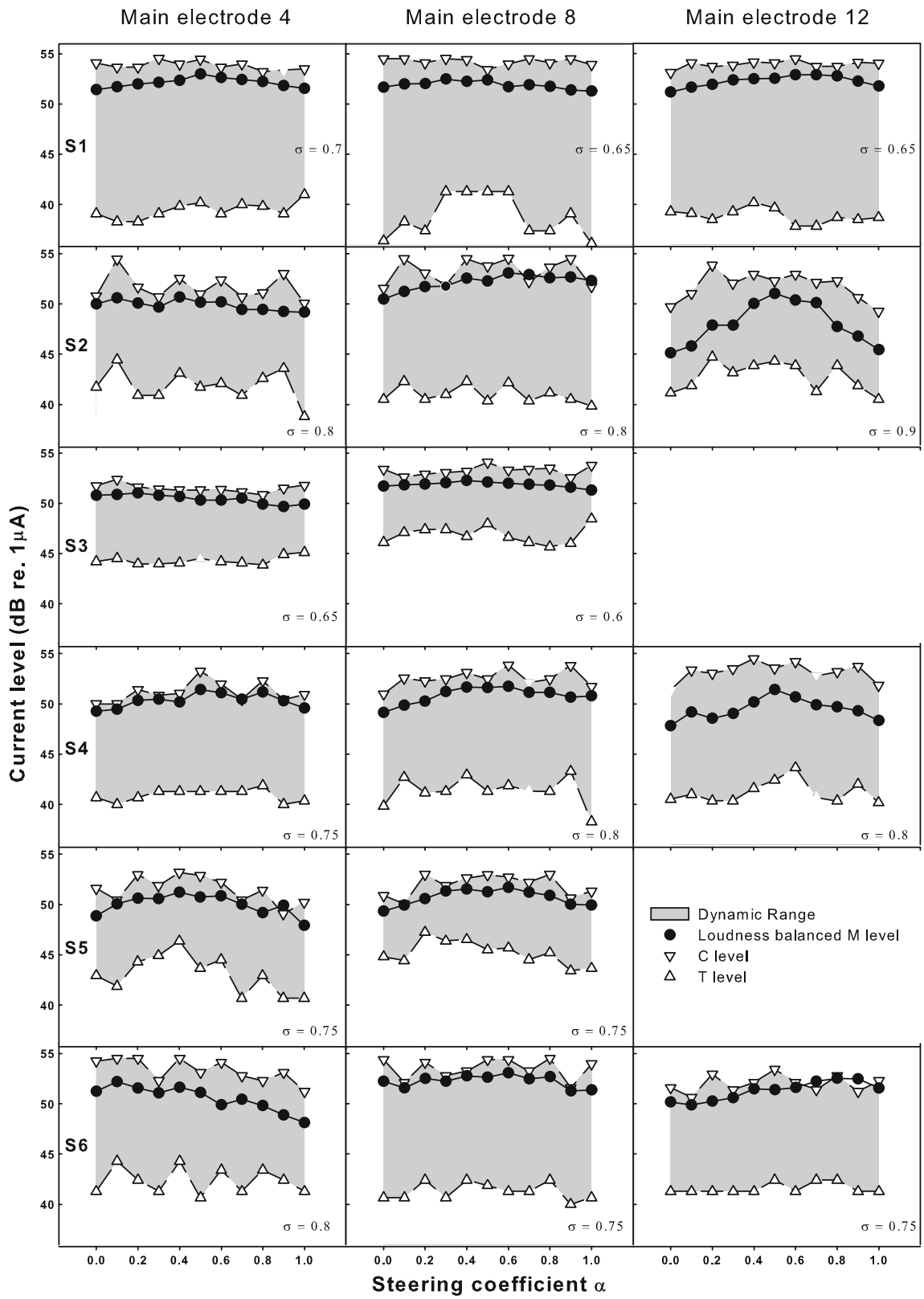

FIG. 8. Thresholds (T-levels: *upward open triangles*), upper loudness limits (C-levels: *downward open triangles*), and loudness-balanced most comfortable levels (M-levels: *solid circles*) as a function of the steering coefficient α for individual subjects (*different rows*) and main electrodes (*different columns*). The dynamic ranges between T/C levels are shown as the *shaded areas*. All current levels are in decibels re 1 μA. The applied compensation coefficient σ is included in each plot.

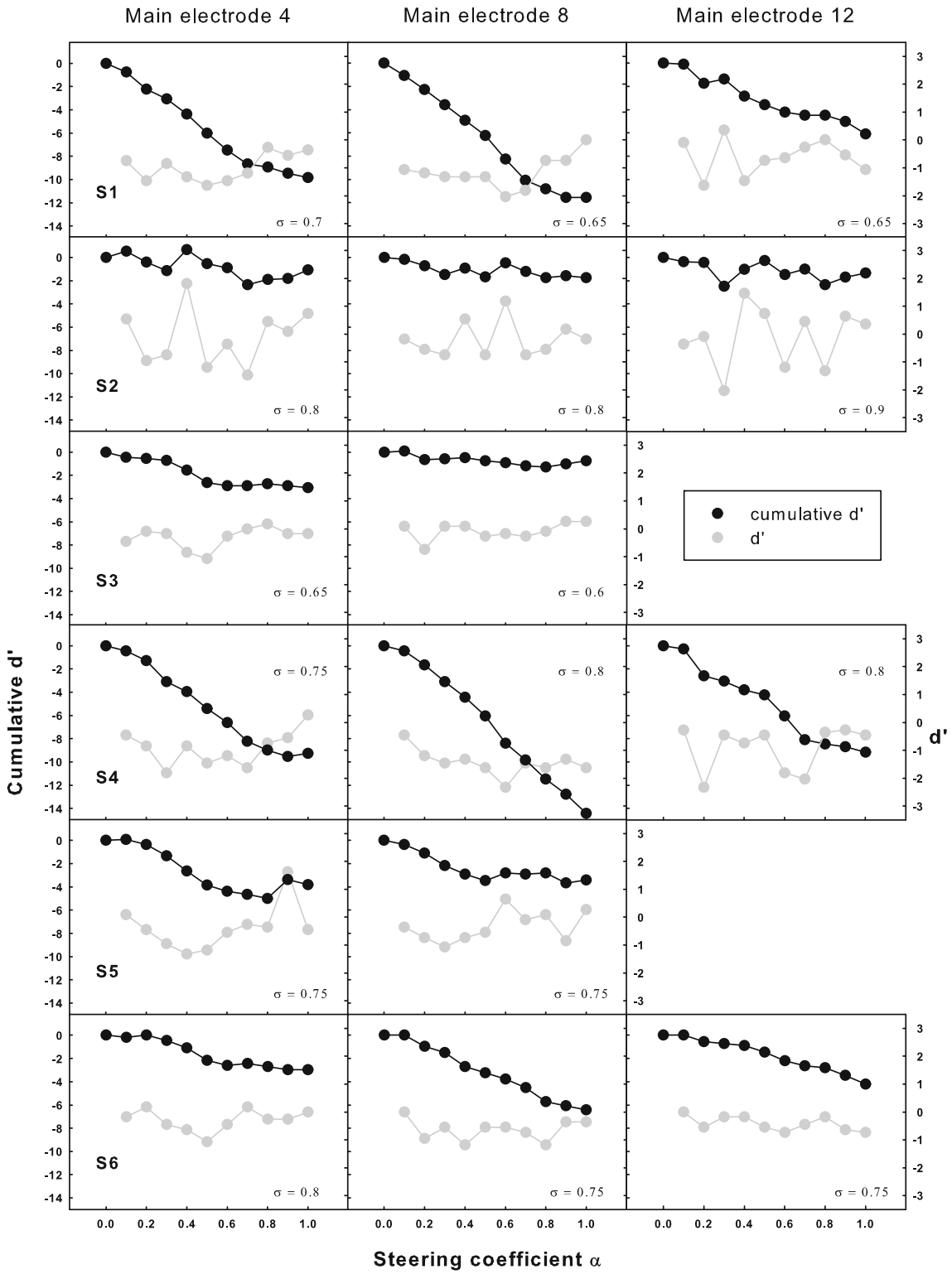

FIG. 9. Cumulative d' from α=0 (*black circles; left ordinate*) and d' values between adjacent α (*gray circles; right ordinate*) for pitch ranking as a function of the steering coefficient α for individual subjects (*different rows*) and main electrodes (*different columns*). The applied compensation coefficient σ is shown in each plot.

cumulative d' (i.e., the cumulative d' at α=1) ranged from −0.74 to −14.42 for different subjects and electrodes with a mean of −7.44. The overall cumulative d' can be converted to the number of discrimina-

ble pitch steps when divided by a d' threshold corresponding to the just-noticeable-difference in pitch (Kwon and van den Honert 2006a). Using the same d' threshold (1.16 or 79.4 % correct in a 2AFC task) as in previous studies such as Donaldson et al. (2005), it was found that steered pTP mode created on average six pitch steps on a main electrode in this study. A one-way RM ANOVA revealed no significant effect of electrode ($F_{2,8}$=0.17, p=0.85) on the overall cumulative d', indicating similar pitch changes with steered pTP stimuli on different main electrodes. The compensation coefficient σ (shown in each plot of Fig. 9) was not correlated with the overall cumulative d' (r^2=0.11, p=0.22); thus, the variable pitch changes across subjects cannot be explained by different degrees of current focusing. Instead, the inter-subject variability in pitch changes may be partially due to different onsets of hearing loss, which can result in different degrees of neural survival. The two pre-lingually deafened subjects (S3 and S5) did have poorer pitch discrimination and less overall cumulative d'.

Discussion

Experiment 1 tested loudness and pitch perception with steered pTP mode on three main electrodes. Although variable across subjects and electrodes, the loudness-balancing data confirmed the hypothesis that steered pTP stimuli with α=0.5 required more current to achieve equal loudness than stimuli with α=0 or 1. As expected, lower pitches were generally perceived with increasing α in the pitch-ranking tests. However, there was no clear evidence that pitch discrimination with steered pTP mode was better for α around 0.5 than for α around 0 or 1, except for some subjects and electrodes.

Subject- and electrode-specific compensation coefficient σ. The highest possible σ values found for individual subjects were in a range (>0.6) that has been shown to generate narrower excitation patterns than σ=0 (MP stimulation) with equal loudness (Bonham and Litvak 2008), and thus should be able to support more effective current steering. Previous studies of pTP mode (e.g., Mens and Berenstein 2005; Litvak et al. 2007; Berenstein et al. 2008) did not attempt to find the highest possible σ and only tried σ values of 0.25, 0.5, or 0.75, which may have underestimated the benefits of current focusing to CI users. Assuming that higher σ values would improve speech perception with more focused stimulation, our results suggest that finer adjustments of σ may be necessary for individual CI users, but not for individual electrodes within each patient. Although it may still be time-consuming, our method for searching the highest possible σ can be useful for such fitting optimization of pTP-mode processing strategies.

Inconsistent patterns of various loudness contours. Measurements of T/C levels for individual subjects and electrodes (Fig. 8) did not show consistent patterns across α as in model predictions (Fig. 5), possibly due to the susceptibility of focused pTP stimulation to variable local electrode–neuron interface, which was not simulated in the basic model. Also, note that the model levels across α were simply assumed to generate equal loudness with the same total number of activated neurons, which may or may not be a valid hypothesis. On the other hand, the measured T/C levels were also not strictly loudness balanced across α using the adaptive procedure because loudness perception at these two levels was either too weak or too strong to be tested. Bierer (2007) found significantly higher thresholds for full TP stimulation (σ=1, α=0.5) compared to full BP stimulation (σ=1, α=0) across the whole electrode array. However, similar T-levels were found for standard pTP (σ<1, α=0.5) and pBP modes (σ<1, α=0 or 1) in this study. The smaller σ or less proportion of intra-cochlear return current may have reduced the T-level differences between standard pTP and pBP modes. Our results also did not show evidence that standard pTP mode would generate larger DRs than pBP mode, at least for the tested σ. The similar DRs across α had implications for a quick yet efficient fitting of steered pTP mode. For example, the DR measured for α=0.5 can be used to estimate the C levels for the other α from the corresponding T levels.

Somewhat similar to model predictions (Fig. 5), the equal-loudness contours at M-level (Fig. 8) for S2, S4, and S5 exhibited higher current requirement for α around 0.5 than for α around 0 and 1, supporting the hypothesis that more focused stimulation of standard pTP mode requires more current to achieve equal loudness than pBP stimulation. For S6, the peaks of M-level contours shifted to α=0 or 1. It is possible that her neural survival was poorer and/or her electrode-neuron distance was longer around one of the flanking electrodes. Thus, more current was required for pBP mode with α=0 or 1, which had a side lobe of excitation near the apical or basal flanking electrode, respectively. The relatively flat M-level contours of S1 and S3 may have been visually compressed because the y-axis of Figure 8 was scaled to show the complete DRs. It also happened that the compensation coefficients σ of S1 and S3 were smaller than those of the other subjects. The variation of M-level contour, quantified by the difference between the maximum and minimum M-levels of each contour, was indeed positively correlated with σ across all subjects and electrodes (Pearson's correlation, r^2=0.66, p<0.001). The moderate correlation suggests that at least for some tested electrodes, higher σ of steered pTP mode required more variable current levels to keep equal loudness perception with different α.

Variable pitch-ranking results across electrodes and α. Figure 9 shows that in general, subjects perceived lower pitches when α increased from 0 to 1, and their pitch discrimination was not better with any specific α value. The lack of significant difference in d' values between α=0.5 (standard pTP mode) and α=0 or 1 (pBP mode) was not consistent with the simplified model predictions. Again, the different local electrode–neuron interfaces of individual electrodes may be a major factor underlying the irregular d' functions. Besides, the α step of 0.1 may have been too small for some subjects to reliably rank the pitches of consecutive pairs of steered pTP stimuli, and this floor effect may have contributed to the variable d' values. A larger α step (e.g., 0.2) may help ease the task of pitch ranking and better estimate the d' values, especially in cases where performance was near chance (i.e., d' close to 0).

The variable pitch-ranking results also exhibited pitch reversals (i.e., higher rather than lower pitches with increasing α), which occurred most often for S2. Pitch reversals with steered pTP mode did not necessarily occur around α=0 or 1, and thus were not caused by the perceptually salient side lobe around the return electrode as in pBP mode or phantom electrode (Saoji and Litvak 2010). It is also unlikely that such pitch reversals were due to the ±0.5-dB amplitude roving used in the pitch-ranking tests because the added random loudness changes across trials should not have consistently reversed pitch ranking. To examine S2's susceptibility to amplitude roving, she was retested on EL8 without amplitude roving. The results (right panel in Fig. 10) did show improved pitch discrimination (or greater negative d' values) between consecutive pairs of steered pTP stimuli than those with amplitude roving (left panel). However, even without amplitude roving, pitch reversals still occurred for different α than with amplitude roving, showing inconsistent pitch judgments. Future measurements of the actual excitation patterns may be necessary to explain the cause of pitch reversals in steered pTP mode.

Comparison with phantom electrodes. Due to the different working principles (i.e., varying the proportion of current on return or main electrodes), the proposed pTP-mode current steering may not be directly comparable with monopolar- or quadrupolar-mode current steering (e.g., Donaldson et al. 2005; Landsberger and Srinivasan 2009). However, it is worth comparing the present results with those of phantom electrodes proposed by Saoji and Litvak (2010). Phantom-electrode stimuli were indeed pBP stimuli with a basal return electrode or $pTP_{ELn,\ \alpha=1}$ in this study. Instead of varying the steering coefficient α, Saoji and Litvak 2010) varied the compensation coefficient σ to control the proportion of current returned to the basal electrode. Similar to our results, their subjects also perceived lower pitches for higher σ (or with more current returned to the basal flanking electrode). However, when σ was 0.6 or higher, many of their subjects were affected by the perceptually salient side lobe and perceived higher instead of lower pitches for higher σ (i.e., pitch reversals). In contrast, as mentioned above, the side lobe effect cannot explain the pitch reversals observed with steered pTP mode in this study. The overall pitch changes created by phantom electrodes were actually similar to those of steered pTP mode. Saoji and Litvak (2010) only tested phantom electrodes with the basal return electrode, and the overall cumulative d' (from σ=0 to the highest σ without pitch reversals) ranged from −2 to −5 for their subjects. If phantom electrodes with the apical return electrode were similarly perceived, the overall cumulative d' would presumably double and match well with those of steered pTP mode in this study.

EXPERIMENT 2: PITCH RANKING OF STEERED PTP STIMULI ON ADJACENT MAIN ELECTRODES

Experiment 1 tested the relative pitch changes with steered pTP stimuli on a main electrode and found that,

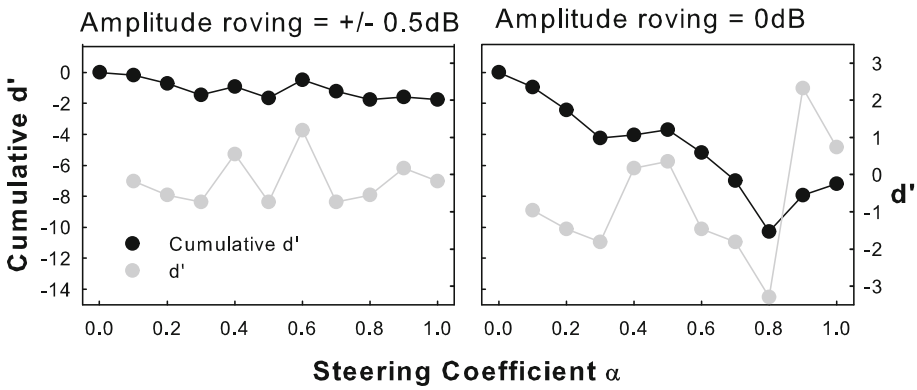

FIG. 10. Pitch-ranking results of subject S2 on EL8 with or without amplitude roving.

in general, pitch monotonically decreased as the steering coefficient α increased from 0 to 1. To implement steered pTP mode along the electrode array, it is important to know if the pitch ranges of adjacent main electrodes both in steered pTP mode would overlap. To answer this question, pitch was compared between steered pTP stimuli on two adjacent main electrodes EL7 and EL8 in experiment 2.

Methods

Subjects and stimuli. Subjects S1, S4, and S6 from experiment 1 participated in experiment 2. These subjects had relatively better pitch discrimination and hardly any pitch reversals with steered pTP mode on EL8 in experiment 1. Their well-perceived pitch ranges from α=0 to α=1 on EL8 and EL7 could thus be reliably compared using the following procedure. Stimuli were the same as those defined in experiment 1.

Loudness balancing and pitch ranking between EL7 and EL8. Loudness balancing and pitch ranking of steered pTP stimuli on EL7 were first tested using the same procedure as in experiment 1, except that the stimuli on EL7 (i.e., $pTP_{EL7,\ \alpha=0}$, $pTP_{EL7,\ \alpha=0.1}$, …, $pTP_{EL7,\ \alpha=1}$) were loudness balanced to $pTP_{EL8,\ \alpha=1}$ at M-level. These tests aimed to confirm that pitch changed in a similar fashion (i.e., lower pitches for higher α) with steered pTP stimuli on both EL7 and EL8.

Based on the tonotopic organization of cochlea, the pitch range on EL8 (from α=0 to α=1) was expected to be higher than that on EL7. To determine if there was overlap between the two pitch ranges, the lowest pitch on EL8 elicited by $pTP_{EL8,\ \alpha=1}$ was compared with the various pitches on EL7, while the highest pitch on EL7 elicited by $pTP_{EL7,\ \alpha=0}$ was compared with the various pitches on EL8. If the lowest-pitch stimulus on EL8 ($pTP_{EL8,\ \alpha=1}$) was perceived as higher in pitch even than the highest-pitch stimulus on EL7 ($pTP_{EL7,\ \alpha=0}$), then the two pitch ranges did not overlap. Otherwise, it was possible to find a stimulus on EL7 ($pTP_{EL7,\ \alpha=\alpha1}$) that was pitch-matched to $pTP_{EL8,\ \alpha=1}$ and a stimulus on EL8 ($pTP_{EL8,\ \alpha=\alpha2}$) that was pitch-matched to $pTP_{EL7,\ \alpha=0}$. In other words, the pitch range between $pTP_{EL8,\ \alpha=\alpha2}$ and $pTP_{EL8,\ \alpha=1}$ overlapped with that between $pTP_{EL7,\ \alpha=0}$ and $pTP_{EL7,\ \alpha=\alpha1}$. Also, with matched pitch percepts, $pTP_{EL7,\ \alpha=\alpha1}$ indicated the apically shifted excitation of $pTP_{EL8,\ \alpha=1}$, while $pTP_{EL8,\ \alpha=\alpha2}$ indicated the basally shifted excitation of $pTP_{EL7,\ \alpha=0}$.

Pitch ranking was tested using the same 2AFC task as in experiment 1. In one test, the reference was $pTP_{EL8,\ \alpha=1}$, and the signal was randomly selected from $pTP_{EL7,\ \alpha=0}$, $pTP_{EL7,\ \alpha=0.1}$, …, and $pTP_{EL7,\ \alpha=1}$. In the other test, the reference was $pTP_{EL7,\ \alpha=0}$, and the signal was randomly selected from $pTP_{EL8,\ \alpha=0}$, $pTP_{EL8,\ \alpha=0.1}$, …, and $pTP_{EL8,\ \alpha=1}$. In each trial, the reference and signal were presented in a random order, and the subject had to judge which stimulus was higher in pitch. Amplitude roving of ±0.5 dB was applied to all stimuli to reduce possible loudness effects. All stimulus pairs were repeated 20 times in a run, and data from two runs were averaged to obtain the percentages that the signals were perceived as higher in pitch than the reference. These scores were fitted with a sigmoid function to estimate the signal that was pitch-matched to the reference.

Results

The cumulative d' for pitch ranking on EL7 is plotted as a function of α in the right column of Figure 11. Similar to that on EL8 (obtained from experiment 1 and re-plotted in the left column), the cumulative d' on EL7 generally decreased as more current was returned to the basal flanking electrode, or when α increased. The overall cumulative d' (i.e., the cumulative d' at α=1) on EL7 was also similar to that on EL8 for each subject. Also note that the highest possible compensation coefficient σ that allowed for full loudness growth within the compliance limit of the implant was identical on the two adjacent main electrodes, as shown in the upper right corner of each plot. This may indicate that for these selected subjects, the adjacent main electrodes EL7 and EL8 had similar neural survival, electrode–neuron distances, and impedances.

Figure 12 shows the pitch-ranking data between steered pTP stimuli on EL7 and EL8. The left column shows the percentages that signals on EL7 were judged as higher in pitch than the reference $pTP_{EL8,\ \alpha=1}$, while the right column shows the percentages that signals on EL8 were judged as higher in pitch than the reference $pTP_{EL7,\ \alpha=0}$. As shown in the left column, the lowest pitch on EL8 elicited by $pTP_{EL8,\ \alpha=1}$ fell in the middle of the pitch range on EL7 (i.e., higher than the pitch of $pTP_{EL7,\ \alpha=1}$ but lower than that of $pTP_{EL7,\ \alpha=0}$). Similarly, in the right column, the highest pitch on EL7 elicited by $pTP_{EL7,\ \alpha=0}$ also fell in the middle of the pitch range on EL8 (i.e., higher than the pitch of $pTP_{EL8,\ \alpha=1}$ but lower than that of $pTP_{EL8,\ \alpha=0}$). The only exception was that S6 did not reliably perceive $pTP_{EL7,\ \alpha=0}$ as lower in pitch than $pTP_{EL8,\ \alpha=0}$. Nevertheless, the results suggest that the pitch ranges of adjacent main electrodes did overlap with each other. Each S-shaped psychometric function in Figure 12 was fitted with a three-parameter sigmoid function:

$$y = \frac{A}{1 + \exp\left(-\frac{x - x_0}{B}\right)}$$

where y is the percentage that the signal was judged as higher in pitch than the reference and x is the α of signal. The best-fit sigmoid functions (all with $r^2 > 0.94$ and $p < 0.005$) are shown by solid curves, and the

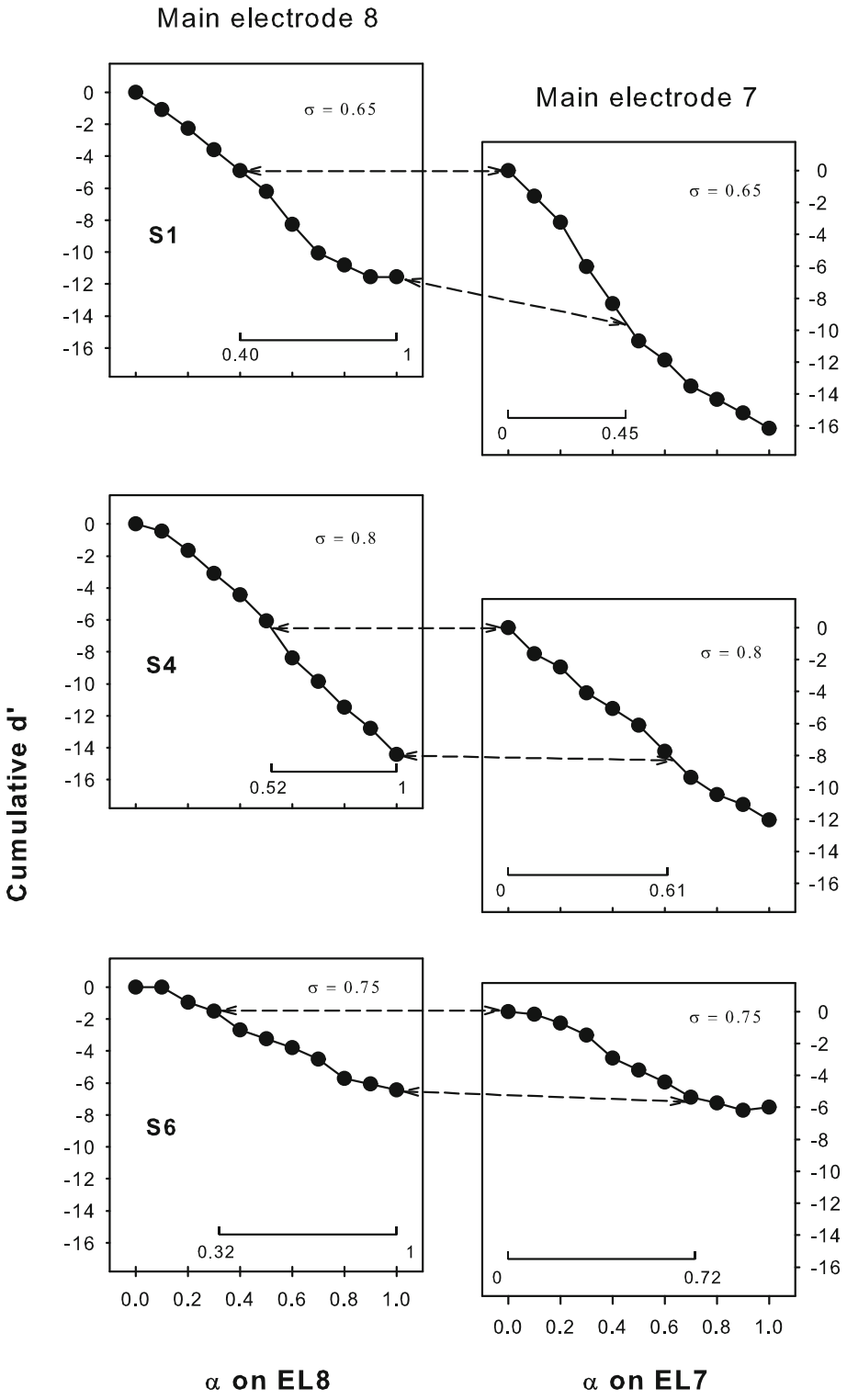

FIG. 11. Cumulative *d'* from α=0 for pitch ranking on EL8 (*left column*; data from experiment 1) and EL7 (*right column*) as a function of the steering coefficient α for subjects S1, S4, and S6. The applied compensation coefficient σ is included in each plot. The pitch-ranking results between the two adjacent main electrodes (shown in Fig. 12) were used to determine their overlapped pitch ranges, which are aligned with each other along the ordinate and connected by the *dashed lines*. The interval of α for the overlapped pitch range is also indicated by the *horizontal line at the bottom of each plot*.

corresponding parameters are included in each plot. The parameter B was in inverse proportion to the slope of the function. The parameter A represented the highest percentage of the function and was near 100 except for S6 with the reference $pTP_{EL7,\ \alpha=0}$. When A was 100, the parameter x_0 represented α of the signal that was pitch-matched to the reference (i.e., with 50 % responses in pitch ranking). For S6 with the reference $pTP_{EL7,\ \alpha=0}$, α of the pitch-matched signal on EL8 was calculated by solving for x with y equal to 50 % responses in the best-fit sigmoid function.

Take S4 for example. Her x_0 parameters showed that $pTP_{EL7,\ \alpha=0}$ was pitch-matched to $pTP_{EL8,\ \alpha=0.52}$, while $pTP_{EL8,\ \alpha=1}$ was pitch-matched to $pTP_{EL7,\ \alpha=0.61}$. In other

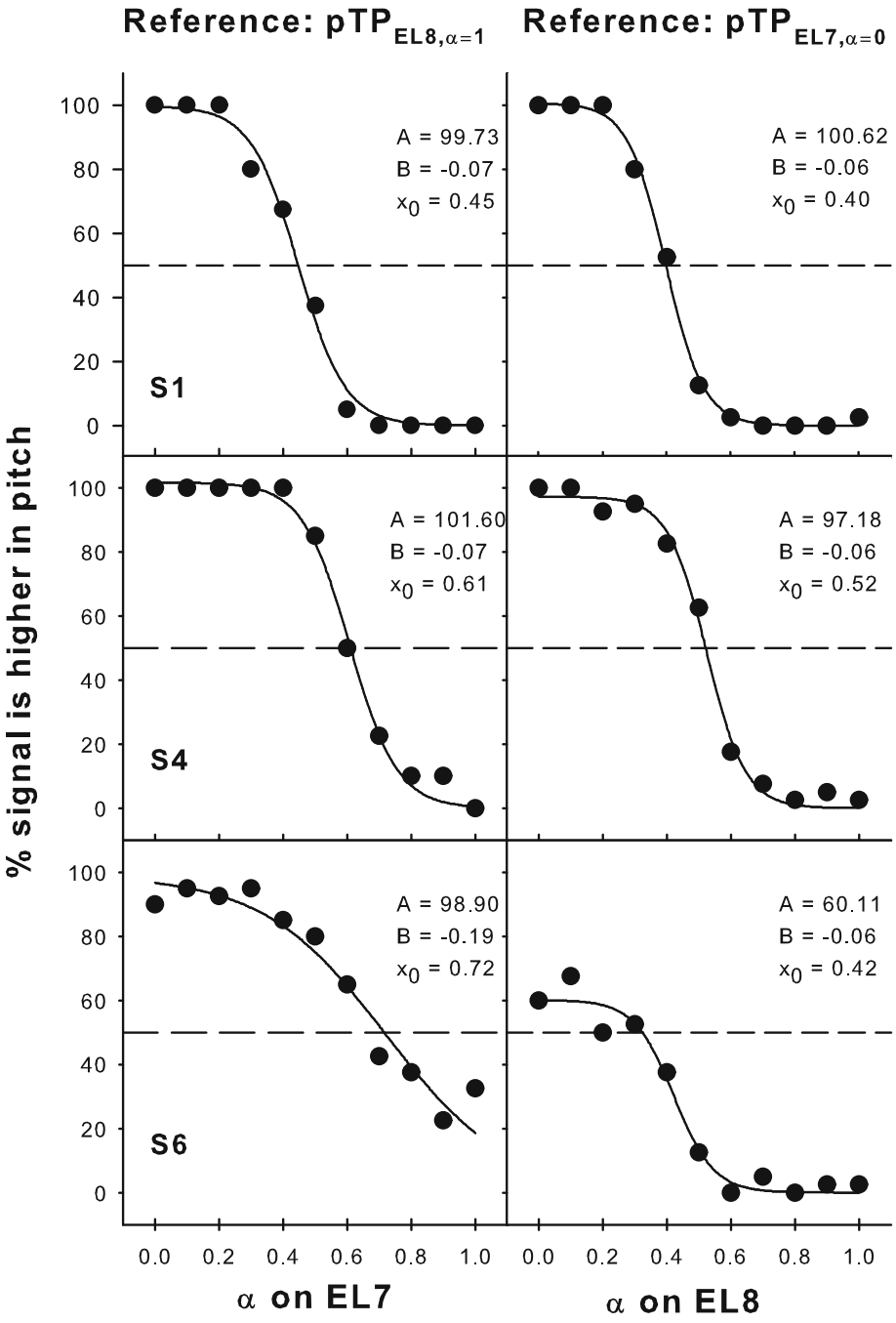

FIG. 12. Pitch-ranking results between EL7 and EL8 for subjects S1, S4, and S6. The *left column* shows the percentages that signals on EL7 ($pTP_{EL7,\ \alpha=0,\ 0.1,\ ...,\ 1}$) were judged as higher in pitch than the lowest-pitch reference on EL8 (i.e., $pTP_{EL8,\ \alpha=1}$). The *right column* shows the percentages that signals on EL8 ($pTP_{EL8,\ \alpha=0,\ 0.1,\ ...,\ 1}$) were judged as higher in pitch than the highest-pitch reference on EL7 (i.e., $pTP_{EL7,\ \alpha=0}$). The *solid curves* show the best-fit sigmoid functions for the data (*solid circles*), with the function parameters indicated in each plot. The *dashed lines* correspond to 50 % responses on the function where the signal and reference were matched in pitch.

words, the pitch range between $pTP_{EL8,\ \alpha=0.52}$ and $pTP_{EL8,\ \alpha=1}$ overlapped with that between $pTP_{EL7,\ \alpha=0}$ and $pTP_{EL7,\ \alpha=0.61}$. The overlapped pitch range was indicated in the second row of Figure 11 by aligning $pTP_{EL7,\ \alpha=0}$ with $pTP_{EL8,\ \alpha=0.52}$ and $pTP_{EL8,\ \alpha=1}$ with $pTP_{EL7,\ \alpha=0.61}$ along the ordinate. The interval of α for the overlapped pitch range was also indicated by the horizontal line at the bottom of each plot. The cumulative d' was calculated within the overlapped pitch range and was similar on EL7 (–7.97) and EL8 (–7.69). Similar results were found for S6. However, for S1, the cumulative d' of the overlapped pitch range was less on EL8 (–6.77) than on EL7 (–9.20). This suggests that the estimated cumulative d' of the same pitch range may differ due to different intermediate stimuli used for d' measurements (Kwon and van den Honert, 2006a). S1's poorer pitch discrimination on EL8 for α from 0.7 to 1 in steps of 0.1 may have underestimated the cumulative d' of the overlapped pitch range.

Discussion

Pitch overlap between adjacent main electrodes. For a subset of better-performing subjects, the lower half of the pitch range on EL8 overlapped with the higher half of the pitch range on EL7. The overlapped pitch

ranges between adjacent main electrodes at the loudness-balanced M-level in these CI subjects were better matched with the model predictions based on the CoG rather than the peak of excitation (Fig. 6). Therefore, place-pitch perception elicited by steered pTP stimuli was more likely determined by the CoG than by the peak of excitation.

Figure 11 shows that, on average, $pTP_{EL8,\ \alpha=1}$ had a similar pitch to $pTP_{EL7,\ \alpha=0.6}$. Their simulated CoGs of excitation were also close together in Figure 6. The excitation pattern of $pTP_{ELn,\ \alpha=0.5}$ was centered on ELn because of its symmetric current return to the two flanking electrodes. When α varied from 0.5 to 1 for steered pTP stimuli on EL8, the CoG of excitation was steered apically from EL8 to EL7 (i.e., a shift of about one physical electrode). Similarly, the average pitch match between $pTP_{EL7,\ \alpha=0}$ and $pTP_{EL8,\ \alpha=0.4}$ suggests that when α varied from 0.5 to 0 for steered pTP stimuli on EL7, the CoG of excitation shifted about one physical electrode basally from EL7 to EL8. Such amounts of CoG shifts were similar to those with phantom electrodes (Saoji and Litvak, 2010). Although pitch ranking was only tested between steered pTP stimuli on EL7 and EL8, similar results were expected for the other electrodes because pitch perception with steered pTP stimuli was not significantly different on different electrodes in experiment 1.

Selection of α range for each main electrode. To implement steered pTP mode along the electrode array in a CI speech processor, the range of steering coefficient α on each electrode should be chosen so that pitch changes continuously from one electrode to the next without overlap. Based on Figures 6 and 11, it is reasonable to assume that on average, the pitch range between $pTP_{EL8,\ \alpha=0.4}$ and $pTP_{EL8,\ \alpha=0.6}$ may overlap with that between $pTP_{EL7,\ \alpha=0}$ and $pTP_{EL7,\ \alpha=0.3}$. Similarly, the pitch range between $pTP_{EL7,\ \alpha=0.4}$ and $pTP_{EL7,\ \alpha=0.6}$ is expected to overlap with that between $pTP_{EL6,\ \alpha=0}$ and $pTP_{EL6,\ \alpha=0.3}$. To elicit continuous non-overlapped pitch changes, one can use α values from 0.4 to 0.6 on each electrode. In this way, pitch decreases as the stimuli change from $pTP_{EL8,\ \alpha=0.4}$ to $pTP_{EL8,\ \alpha=0.6}$, continues to decrease as the stimuli change from $pTP_{EL7,\ \alpha=0.4}$ to $pTP_{EL7,\ \alpha=0.6}$, and so on. On the other hand, instead of using the same α range from 0.4 to 0.6 on each electrode, one can use a wider α range on the electrode with better pitch discrimination and more discriminable pitch steps than its adjacent electrode. This alternative selection of α range may provide more spectral resolution but requires sophisticated pitch tests during fitting.

GENERAL DISCUSSION AND SUMMARY

Loudness and pitch perception with steered pTP mode was predicted using model simulations and tested in psychophysical experiments. Although CI subjects had similar T/C levels and dynamic ranges across α on a main electrode, their loudness-balanced M-levels were significantly higher with α=0.5 than with α=0 or 1. This is consistent with the model prediction that more current is required for more focused standard pTP mode (α=0.5) than for less focused pBP mode (α=0 and 1) to achieve equal loudness. CI subjects generally perceived lower pitches (with an average overall cumulative d' of −7) as α increased from 0 to 1. However, their pitch discrimination was not better with α around 0.5 (i.e., more focused standard pTP mode) than with α around 0 or 1 (i.e., less focused pBP mode), except for some subjects and electrodes. For three better-performing CI subjects, pitch comparisons between steered pTP stimuli on adjacent main electrodes showed that about half of the pitch ranges of EL7 and EL8 overlapped with each other (e.g., the lower half of EL8 matched with the higher half of EL7). Compared with the model predictions, these results suggest that pitch changes elicited by steered pTP stimuli were largely driven by the shifted CoG rather than by the peak of excitation.

The small heterogeneous subject group (i.e., N=6 with two being pre-lingually deafened) may not be ideal for this proof-of-concept study. The inter-subject variability in loudness and pitch perception was high, which unfortunately weakened the overall findings of this study and made the results somewhat anecdotal. The underlying reasons for inter-subject variability were unclear, but individual subjects' different electrode–neuron interfaces and various onsets of hearing loss (i.e., pre- or post-lingually deafened) most likely contributed to their different performances. In future studies, variations in electrode–neuron distance and neural survival will be introduced to the computational model to predict their effects on loudness and pitch perception with steered pTP mode. A more straightforward way to explain the variable perceptual data is to directly estimate the excitation patterns of steered pTP stimuli with different α in each subject. This can be achieved by measuring the forward masking patterns of steered pTP stimuli using psychophysical methods (e.g., Chatterjee and Shannon 1998; Kwon and van den Honert 2006b; Srinivasan et al. 2010; Landsberger et al. 2012) or using electrically evoked compound action potentials (e.g., Cohen et al. 2003; Hughes and Stille 2008).

In summary, both the model and psychophysical data verified the feasibility and efficacy of pTP-mode current steering, which can be readily incorporated into the pTP-mode processing strategies (e.g., Berenstein et al. 2008) to improve CI performance. For example, Bierer and Faulkner (2010) argued that with the more focused standard pTP mode, CI users were more susceptible to cochlear "dead regions," which required more current

to reach T/C levels and had less spatial selectivity of electric stimulation. In such a case, an α value different from 0.5 may be used to steer pTP stimuli away from the dead region to more efficiently transmit the corresponding spectral information. In addition, as discussed in experiment 2, α values from 0.4 to 0.6 can be applied to steered pTP stimuli on each main electrode to create additional frequency channels and encode fine spectral details. The long pulse phase duration (226 μs) in this study helped achieve full loudness growth with steered pTP mode, but may limit the stimulation rate available in CI processors. As suggested by Landsberger and Srinivasan (2009), this issue may be partially addressed by using an n-of-m strategy that only stimulates a subset of largest-amplitude channels in each cycle. The proposed idea of combining current steering with focusing (see also Landsberger and Srinivasan 2009) may provide CI users with more distinctive pitches and frequency channels than MP-mode current steering in the HiRes-120 strategy. Future studies will implement pTP-mode current steering in multi-channel CI speech processors and test the potential benefits to CI users using appropriate psychophysical, speech, and music tests.

ACKNOWLEDGMENTS

We are grateful to all the subjects for their participation in the experiments. We thank Dr. Richard Miyamoto, Dr. Tonya Bergeson-Dana, and the cochlear implant team at the Indiana University School of Medicine for help in recruiting participants. We also thank Dr. Joshua Goldwyn for providing the Matlab code of the computational model. Research was supported in part by NIH (R21-DC-011844) and by Purdue Research Foundation. The Associate Editor Dr. Joseph Hall and three anonymous reviewers provided helpful comments on an earlier version of the manuscript.

REFERENCES

BERENSTEIN CK, MENS LHM, MULDER JJS, VANPOUCKE FJ (2008) Current steering and current focusing in cochlear implants: comparison of monopolar, tripolar, and virtual channel electrode configurations. Ear Hear 29:250–260

BIERER JA (2007) Threshold and channel interaction in cochlear implant users: evaluation of the tripolar electrode configuration. J Acoust Soc Am 121:1642–1653

BIERER JA (2010) Probing the electrode-neuron interface with focused cochlear implant stimulation. Trends Amplif 14:84–95

BIERER JA, FAULKNER KF (2010) Identifying cochlear implant channels with poor electrode-neuron interface: partial tripolar, single-channel thresholds and psychophysical tuning curves. Ear Hear 31:247–258

BIERER JA, MIDDLEBROOKS JC (2002) Auditory cortical images of cochlear-implant stimuli: dependence on electrode configuration. J Neurophysiol 87:478–492

BIERER JA, MIDDLEBROOKS JC (2004) Cortical responses to cochlear implant stimulation: channel interactions. J Assoc Res Otolaryngol 5:32–48

BONHAM BH, LITVAK LM (2008) Current focusing and steering: modeling, physiology, and psychophysics. Hear Res 242:141–153

CHATTERJEE M, SHANNON RV (1998) Forward masked excitation patterns in multielectrode electrical stimulation. J Acoust Soc Am 103:2565–2572

COHEN LT, RICHARDSON LM, SAUNDERS E, COWAN RSC (2003) Spatial spread of neural excitation in cochlear implant recipients: comparison of improved ECAP method and psychophysical forward masking. Hear Res 179:72–87

CORMEN TH, LEISERSON CE, RIVEST RL, STEIN C (2009) Binary search tree. In: Introduction to Algorithms, 3rd edn. MIT Press, Cambridge, pp 286-299.

DONALDSON GS, KREFT HA, LITVAK LM (2005) Place-pitch discrimination of single- versus dual-electrode stimuli by cochlear implant users. J Acoust Soc Am 118:623–626

FINLEY CC, SKINNER MW (2008) Role of electrode placement as a contributor to variability in cochlear implant outcomes. Otol Neurotol 29:920–928

FIRSZT JB, HOLDEN LK, REEDER RM, SKINNER MW (2009) Speech recognition in cochlear implant recipients: comparison of standard HiRes and HiRes 120 sound processing. Otol Neurotol 30:146–152

GOLDWYN JH, BIERER SM, BIERER JA (2010) Modeling the electrode–neuron interface of cochlear implants: effects of neural survival, electrode placement, and the partial tripolar configuration. Hear Res 268:93–104

HACKER MJ, RATCLIFF R (1979) A revised table of d' for M-alternative forced choice. Percept Psychophys 26:168–170

HUGHES ML, STILLE LJ (2008) Psychophysical versus physiological spatial forward masking and the relation to speech perception in cochlear implants. Ear Hear 29:435–452

JESTEADT W (1980) An adaptive procedure for subjective judgments. Atten Percept Psychophys 28:85–88

KRAL A, HARTMANN R, MORTAZAVI D, KLINKE R (1998) Spatial resolution of cochlear implants: the electrical field and excitation of auditory afferents. Hear Res 121:11–28

KWON BJ, VAN DEN HONERT C (2006A) Dual-electrode pitch discrimination with sequential interleaved stimulation by cochlear implant users. J Acoust Soc Am 120:EL1–EL6

KWON BJ, VAN DEN HONERT C (2006B) Effect of electrode configuration on psychophysical forward masking in cochlear implant listeners. J Acoust Soc Am 119:2994–3002

LANDSBERGER DM, PADILLA M, SRINIVASAN AG (2012) Reducing current spread using current focusing in cochlear implant users. Hear Res 284:16–24

LANDSBERGER DM, SRINIVASAN AG (2009) Virtual channel discrimination is improved by current focusing in cochlear implant recipients. Hear Res 254:34–41

LITVAK LM, SPAHR AJ, EMADI G (2007) Loudness growth observed under partially tripolar stimulation: model and data from cochlear implant listeners. J Acoust Soc Am 122:967–981

MENS LHM, BERENSTEIN CK (2005) Speech perception with mono- and quadrupolar electrode configurations: a crossover study. Otol Neurotol 26:957–964

MILLER CA, ABBAS P, ROBINSON B, RUBINSTEIN JT, MATSUOKA A (1999) Electrically evoked single fiber action potentials from cat: responses to monopolar, monophasic stimulation. Hear Res 242:184–197

NADOL JB JR, SHIAO JY, BURGESS BJ, KETTEN DR, EDDINGTON DK, GANTZ BJ, KOS I, MONTANDON P, COKER NJ, ROLAND JT JR, SHALLOP JK (2001) Histopathology of cochlear implants in humans. Ann Otol Rhinol Laryngol 110:883–891

Qin MK, Oxenham AJ (2005) Effects of envelope-vocoder processing on F0 discrimination and concurrent-vowel identification. Ear Hear 26:451–460

Rattay F (1999) The basic mechanism for the electrical stimulation of the nervous system. Neurosci 89:335–346

Saoji AA, Litvak LM (2010) Use of "phantom electrode" technique to extend the range of pitches available through a cochlear implant. Ear Hear 31:693–701

Snyder RL, Bierer JA, Middlebrooks JC (2004) Topographic spread of inferior colliculus activation in response to acoustic and intracochlear electric stimulation. J Assoc Res Otolaryngol 5:305–322

Srinivasan AG, Landsberger DM, Shannon RV (2010) Current focusing sharpens local peaks of excitation in cochlear implant stimulation. Hear Res 270:89–100

Zeng FG (2004) Trends in cochlear implants. Trends Amplif 8:1–34